CHARLES UNIVERSITY IN PRAGUE
FACULTY OF MATHEMATICS AND PHYSICS

RELATIVISTIC DISCS AROUND COMPACT OBJECTS

Abstract of Doctoral Thesis

Branch: F-1 – Theoretical Physics, Astronomy and Astrophysics
Supervisor: Prof. RNDr. Zdeněk Stuchlík, CSc.

PETR SLANÝ

AUGUST 2005

UNIVERZITA KARLOVA V PRAZE
MATEMATICKO-FYZIKÁLNÍ FAKULTA

RELATIVISTICKÉ DISKY KOLEM KOMPAKTNÍCH OBJEKTŮ

Autoreferát disertační práce

Obor: F-1 – Teoretická fyzika, astronomie a astrofyzika
Školitel: Prof. RNDr. Zdeněk Stuchlík, CSc.

PETR SLANÝ

SRPEN 2005

Doktorand: Mgr. Petr Slaný

Ústav fyziky
Filozoficko-přírodovědecká fakulta
Slezská univerzita v Opavě
Bezručovo nám. 13
746 01 Opava

Školitel: Prof. RNDr. Zdeněk Stuchlík, CSc.

Školicí pracoviště: Slezská univerzita v Opavě
Filozoficko-přírodovědecká fakulta
Ústav fyziky
Bezručovo nám. 13
746 01 Opava

Oponenti: Prof. RNDr. Jan Novotný, CSc.

Katedra obecné fyziky
Přírodovědecká fakulta Masarykovy univerzity
Kotlářská 2
611 37 Brno

Doc. RNDr. Vladimír Karas, DrSc.

Astronomický ústav AV ČR Praha
Boční II/1401
141 31 Praha 4

Předseda oborové rady F1: Prof. RNDr. Jiří Bičák, DrSc.

Ústav teoretické fyziky
Matematicko-fyzikální fakulta Univerzity Karlovy
V Holešovičkách 2
180 00 Praha 8

Výsledky tvořící disertační práci byly získány během kombinovaného doktorského studia na Matematicko-fyzikální fakultě Univerzity Karlovy v Praze v letech 1997–2005.

Autoreferát byl rozeslán dne 27. srpna 2005.

Obhajoba se koná dne 27. září 2005 v 11.00 hodin před komisí pro obhajoby disertačních prací v oboru *F-1 – Teoretická fyzika, astronomie a astrofyzika* v budově MFF UK, V Holešovičkách 2, 180 00 Praha 8, v posluchárně ÚTF č. 1119.

S disertací je možno se seznámit na studijním oddělení Matematicko-fyzikální fakulty Univerzity Karlovy, Ke Karlovu 3, 121 16 Praha 2.

Contents

The thesis and this abstract (in PDF) are available from author's home page
`http://www.fpf.slu.cz/~sla10uf/thesis/`

Introduction

Quasars, and active galactic nuclei (AGN) in general, belong among the most energetic sources in the Universe. The most probably, power engines of AGN are accretion discs around central supermassive (10^6–$10^{10} M_\odot$) black holes [12, 13]. Scaled-down versions of the AGN phenomena are observed in some powerful galactic X-ray sources called microquasars, in which a stellar-mass black hole accretes matter from its companion in a close binary system [26].

According to the cosmic censorship hypothesis [28] and the uniqueness theorems for black holes [16], the result of the gravitational collapse of a sufficiently massive rotating object is a rotating Kerr black hole, rather than a Kerr naked singularity; further the laws of black-hole thermodynamics forbid conversion of black holes into a naked singularity [18]. However, although the cosmic censorship is a very plausible hypothesis, there is some evidence against it. Naked singularities arise in various models of spherically symmetric collapse (e.g. [22]). In modeling collapse of rotating stars, it was pointed out that although mass shedding and gravitational radiation will reduce the angular momentum of the star during collapse, it will not in general be reduced to the value that corresponds to a Kerr black hole [24,25]. Because cosmic censorship hypothesis is far from being proved, naked singularity spacetimes related to the black-hole spacetimes with a non-zero rotational parameter and/or charge could still be considered conceivable models of, at least, the most energetic AGN and deserve some attention. Of particular interest are those effects that could distinguish a naked singularity from black holes.

Recent data from a wide variety of independent cosmological tests indicate convincingly that in the framework of inflationary cosmology a non-zero, although very small, vacuum energy density, i.e., a relict repulsive cosmological constant, $\Lambda > 0$, or some similarly acting new kind of matter called *quintessence*, has to be invoked in order to explain the dynamics of the recent Universe [8, 20]. Both possibilities are often referred as a *dark energy* in the Universe.

It is well known that the repulsive cosmological constant strongly influences expansion of the Universe, leading finally to an exponentially accelerated stage. However, surprisingly enough, the repulsive cosmological constant could be relevant also in astrophysical processes like the disc accretion in AGN.

Basic properties of geometrically thin accretion discs with low accretion rates and negligible pressure are given by the circular geodesic motion in the black-hole backgrounds [27], while for geometrically thick accretion discs with high accretion rates and pressure being relevant they are determined by equipotential surfaces of test perfect fluid rotating in the background (see, e.g., [1]).

The presented thesis consists of the commented series of four original papers related to some problems of the theory of accretion discs, being written in collaboration with

Prof. Zdeněk Stuchlík and other colleagues:

[I] Z. Stuchlík, P. Slaný and S. Hledík: *Equilibrium configurations of perfect fluid orbiting Schwarzschild–de Sitter black holes*, Astronomy and Astrophysics **363**, 425 (2000).

[II] Z. Stuchlík and P. Slaný: *Equatorial circular orbits in the Kerr–de Sitter spacetimes*, Physical Review D **69**, 064001 (2004).

[III] P. Slaný and Z. Stuchlík: *Relativistic thick discs in the Kerr–de Sitter backgrounds*, Classical and Quantum Gravity **22**, 3623 (2005), *in press*.

[IV] Z. Stuchlík, P. Slaný, G. Török and M. A. Abramowicz: *Aschenbach effect: Unexpected topology changes in the motion of particles and fluids orbiting rapidly rotating Kerr black holes*, Physical Review D **71**, 024037 (2005).

In Section 1 and papers [**I**–**III**], influence of a cosmic repulsion, represented by positive value of the cosmological constant Λ, on accretion processes in black-hole (naked-singularity) backgrounds is analyzed. Moreover, the case of an attractive cosmological constant, $\Lambda < 0$, is also discussed in papers [**I**] (fully) and [**II**] (partly). In Section 2 and paper [**IV**], the *Aschenbach effect* residing in non-monotonic behaviour of the orbital velocity related to locally non-rotating frames (LNRF), as discovered by Aschenbach in the case of Keplerian motion of test particles around rapidly rotating Kerr black holes [7], is discussed. We show that there is a corresponding behaviour of the orbital velocity relative to the LNRF also for non-Keplerian motion of test perfect fluid in thick discs with uniform distribution of the specific angular momentum, $\ell(r, \theta) = \text{const}$.

1

Influence of a repulsive cosmological constant on accretion discs

Various cosmological observations indicate the current value of the vacuum/dark energy density [31]

$$\varrho_{\mathrm{vac}(0)} \approx 0.73 \varrho_{\mathrm{crit}(0)}, \tag{1.1}$$

where the present value of the critical energy density $\varrho_{\mathrm{crit}(0)}$ is related with the Hubble parameter H_0 by[1]

$$\varrho_{\mathrm{crit}(0)} = \frac{3H_0^2}{8\pi}, \quad H_0 = 100h \text{ km s}^{-1} \text{ Mpc}^{-1}. \tag{1.2}$$

Taking value of the dimensionless parameter $h \approx 0.7$, we obtain the relic repulsive cosmological constant to be

$$\Lambda_0 = 8\pi\varrho_{\mathrm{vac}(0)} \approx 1.3 \times 10^{-56} \text{ cm}^{-2}. \tag{1.3}$$

The presence of $\Lambda > 0$ substantially changes the asymptotic structure of black-hole spacetimes, as these become asymptotically de Sitter, not flat spacetimes. In such spacetimes, an event horizon always exists behind which the geometry is dynamic; we call it a cosmological horizon. In the framework of Schwarzschild–de Sitter (SdS) and Kerr–de Sitter (KdS) spacetimes, the equatorial circular motion of test particles (Keplerian motion) and the toroidal equilibrium configurations of barotropic test perfect fluid orbiting with uniform distribution of the specific angular momentum are studied.

1.1 Thin discs

Basic properties of thin discs in both SdS and KdS backgrounds are determined by the equatorial circular motion of test particles because in rotating, KdS backgrounds any tilted disc will be driven to the equatorial plane due to the dragging of inertial frames, as was shown by Bardeen and Petterson in the case of Kerr backgrounds [10].

The motion of a test particle with rest mass m is given by the geodesic equations. In a separated and integrated form, the equations were obtained by Carter [16]. For the

[1] Geometric units $c = G = 1$ are used hereafter.

motion restricted to the equatorial plane ($\mathrm{d}\theta/\mathrm{d}\lambda = 0$, $\theta = \pi/2$) the Carter equations take, in the standard Boyer–Lindquist coordinates (t, r, θ, φ), the following form:

$$r^2 \frac{\mathrm{d}r}{\mathrm{d}\lambda} = \pm R^{1/2}(r), \tag{1.4}$$

$$r^2 \frac{\mathrm{d}\varphi}{\mathrm{d}\lambda} = -I P_\theta + \frac{a I P_r}{\Delta_r}, \tag{1.5}$$

$$r^2 \frac{\mathrm{d}t}{\mathrm{d}\lambda} = -a I P_\theta + \frac{(r^2 + a^2) I P_r}{\Delta_r}, \tag{1.6}$$

where

$$R(r) = P_r^2 - \Delta_r \left(m^2 r^2 + K\right), \tag{1.7}$$

$$P_r = I\mathcal{E}\left(r^2 + a^2\right) - I a \Phi, \quad P_\theta = I(a\mathcal{E} - \Phi), \tag{1.8}$$

$$\Delta_r = r^2 - 2Mr + a^2 - \frac{1}{3}\Lambda r^2\left(r^2 + a^2\right), \quad I = 1 + \frac{1}{3}\Lambda a^2, \tag{1.9}$$

$$K = I^2(a\mathcal{E} - \Phi)^2. \tag{1.10}$$

Here, M is the mass parameter of the background and a is its rotational parameter; in SdS spacetimes, $a = 0$. It is convenient to introduce a dimensionless *cosmological parameter*

$$y = \frac{1}{3}\Lambda M^2 \tag{1.11}$$

and put $M = 1$ to get completely dimensionless formulae, hereafter. The proper time of the particle τ is related to the affine parameter λ by $\tau = m\lambda$. The constants of the motion are: rest mass (m), energy ($\mathcal{E}$), related to the stationarity of the geometry, axial angular momentum (Φ), related to the axial symmetry of the geometry, and "total" angular momentum (K), related to the hidden symmetry of the geometry. For the equatorial motion, K is restricted through Eq. (1.10) following from the conditions on the latitudinal motion [33]. Notice that $\mathcal{E}$ and Φ cannot be interpreted as energy and axial angular momentum at radial infinity, since the spacetime is not asymptotically flat.

Specific energy and specific angular momentum are defined by the relations [33]

$$E \equiv \frac{I\mathcal{E}}{m}, \quad L \equiv \frac{I\Phi}{m}. \tag{1.12}$$

The equatorial motion is governed by an "effective potential" given by the condition $R(r) = 0$ for turning points of the radial motion. To get very simple form of the effective potential, it is useful to redefine the axial angular momentum by the relation

$$X \equiv L - aE. \tag{1.13}$$

With the constant of motion X, instead of L, the effective potential takes the form

$$E_{(+)}(r;\ X,\ a,\ y) \equiv \frac{1}{r^2}\left[aX + \Delta_r^{1/2}\left(r^2 + X^2\right)^{1/2}\right]. \tag{1.14}$$

In the stationary regions ($\Delta_r \geq 0$), the motion is allowed where [9]

$$E \geq E_{(+)}(r;\ X,\ a,\ y). \tag{1.15}$$

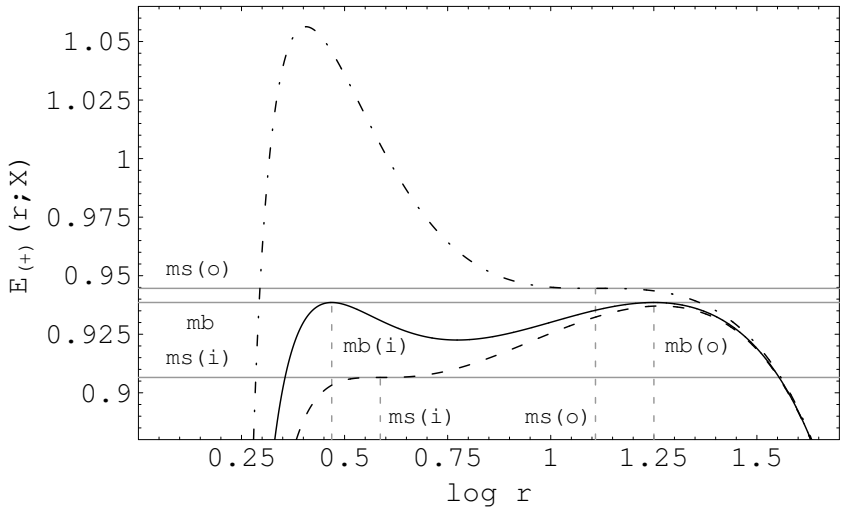

Figure 1.1: Effective potential of the equatorial radial motion of test particles in an appropriately chosen KdS black-hole background ($y = 10^{-4}$, $a^2 = 1.05$). Marginally bound (mb) orbits are given by the solid curve with two local maxima of the same value corresponding to the inner [mb(i)] and outer [mb(o)] marginally bound orbit. The dashed/dashed-dotted effective potential defines the inner/outer marginally stable orbit [ms(i)/ms(o)] by coalescing the local minimum and the (inner/outer) local maximum.

In the black-hole backgrounds, we restrict our attention to the stationary region between the (outer) black-hole and cosmological horizon. In paper [**II**] is shown that black holes (BH) can exist only in the KdS spacetimes with parameters $y \leq y_{\mathrm{c(KdS)}} \doteq 0.059$ or $a^2 \leq a^2_{\mathrm{crit}} \doteq 1.212$. Naked singularities (NS) can exist for any cosmological parameter y, if the rotational parameter a is appropriately chosen. Critical (maximum) value of the cosmological parameter admitting black holes in SdS spacetimes corresponds to $y_{\mathrm{c(SdS)}} = 1/27 \doteq 0.037$ [34]. Typical behaviour of the effective potential in SdS or KdS backgrounds allowing stable circular orbits is presented in Figure 1.1.

The equatorial circular orbits correspond to the local extrema of the effective potential $E_{(+)}(r;\, X,\, a,\, y)$, and can be determined by solving simultaneously the equations $R(r) = 0$, $\mathrm{d}R/\mathrm{d}r = 0$. The specific energy and the specific angular momentum of particles on such orbits are determined by the relations

$$E_{\pm}(r;\, a,\, y) = \frac{1 - \frac{2}{r} - \left(r^2 + a^2\right) y \pm a \left(\frac{1}{r^3} - y\right)^{1/2}}{\left[1 - \frac{3}{r} - a^2 y \pm 2a \left(\frac{1}{r^3} - y\right)^{1/2}\right]^{1/2}}, \tag{1.16}$$

$$L_{\pm}(r;\, a,\, y) = -\frac{2a + ar\left(r^2 + a^2\right) y \mp r\left(r^2 + a^2\right)\left(\frac{1}{r^3} - y\right)^{1/2}}{r\left[1 - \frac{3}{r} - a^2 y \pm 2a \left(\frac{1}{r^3} - y\right)^{1/2}\right]^{1/2}}, \tag{1.17}$$

revealing, in general, the existence of two families of circular orbits. We call them "plus-family" orbits and "minus-family" orbits according to the $\pm$ sign in the relations (1.16)–(1.17). Note that the relations (1.14)–(1.17) are valid for a repulsive cosmological constant ($y > 0$) as well as an attractive cosmological constant ($y < 0$). However, here

we concentrate on the asymptotically de Sitter spacetimes only, i.e., $y > 0$. Corresponding relations for the specific energy and the specific angular momentum of a particle on the equatorial circular orbit in the SdS background follow from the relations (1.16)–(1.17) in the limit $a \to 0$. In SdS backgrounds, just one family of circular orbits exists.

Inspecting expressions (1.16) and (1.17), we find two reality restrictions on the existence of circular orbits. The first one is given by the relation

$$y \leq y_{\rm s} \equiv \frac{1}{r^3}, \tag{1.18}$$

which introduces the notion of the "static radius", given by the formula $r_{\rm s} = y^{-1/3}$ independently of the rotational parameter a. Thus, formally identical result also holds in the SdS backgrounds. The only non-zero component of the 4-velocity of a particle freely moving on the equatorial circular orbit $r = r_{\rm s}$ is the time-component U^t. Note that the position on the static radius is unstable relative to radial perturbations. The second restriction is given by the condition

$$1 - \frac{3}{r} - a^2 y \pm 2a \left(\frac{1}{r^3} - y\right)^{1/2} \geq 0; \tag{1.19}$$

the equality determines radii of photon circular orbits, as both $E \to \infty$ and $L \to \pm\infty$ there. In SdS spacetimes, the photon circular orbit is located at $r = 3$ independently of the cosmological parameter y.

Minus-family orbits exist only in the KdS spacetimes with parameters $y < y_{\rm c(SdS)}$ and $a^2 \leq a^2_{\rm c(s)} \equiv (1 - 3y^{1/3})/y$, in the region $r_{\rm ph-} < r < r_{\rm s}$, where $r_{\rm ph-}$ corresponds to the counterrotating photon circular orbit (its location depends on the parameters y, a of the spacetime), $r_{\rm s}$ is the static radius. Plus-family orbits exist in all KdS spacetimes. In the backgrounds admitting minus-family orbits, the plus-family orbits exist in the region $r_{\rm ph+} < r < r_{\rm s}$ (BH), where $r_{\rm ph+}$ corresponds to the corotating photon circular orbit (its location again depends on the spacetime parameters y, a), or $0 < r < r_{\rm s}$ (NS). Both families coincide at the static radius. In the backgrounds not-admitting minus-family orbits, the upper limit for the existence of plus-family orbits is given by the counterrotating photon circular orbit.

Since the KdS background is not asymptotically flat, the orientation of circular orbits can be related to locally non-rotating frames (LNRF) only. Note that in Kerr backgrounds, orientation of orbits related to LNRF is the same as the one determined from the point of view of stationary observers at infinity. LNRF in the equatorial plane ($\theta = \pi/2$) are defined by the tetrad of 1-forms [35]

$$\omega^{(t)} \equiv \left(\frac{\Delta_r r^2}{I^2 A}\right)^{1/2} {\rm d}t, \quad \omega^{(\varphi)} \equiv \left(\frac{A}{I^2 r^2}\right)^{1/2} ({\rm d}\varphi - \Omega_{\rm LNRF}\, {\rm d}t), \tag{1.20}$$

$$\omega^{(r)} \equiv \left(\frac{r^2}{\Delta_r}\right)^{1/2} {\rm d}r, \qquad \omega^{(\theta)} \equiv r\,{\rm d}\theta, \tag{1.21}$$

with the angular velocity of the LNRF being given by

$$\Omega_{\rm LNRF} \equiv \frac{{\rm d}\varphi}{{\rm d}t} = \frac{a}{A}\Big[(r^2 + a^2) - \Delta_r\Big]; \quad A = (r^2 + a^2)^2 - a^2 \Delta_r. \tag{1.22}$$

Locally measured azimuthal component of particle's 4-momentum in the LNRF is given by its projection onto the 1-form $\omega^{(\varphi)}$: $p^{(\varphi)} = p^{\mu}\omega^{(\varphi)}_{\mu}$, where $p^{\mu} = \mathrm{d}x^{\mu}/\mathrm{d}\lambda$. A simple calculation reveals the intuitively anticipated relation

$$p^{(\varphi)} = \frac{mr}{A^{1/2}}L\,. \tag{1.23}$$

We can see that the sign of $p^{(\varphi)}$ in the LNRF is given by the sign of the specific angular momentum of a particle on the orbit of interest. Therefore the circular orbits with $p^{(\varphi)} > 0,\ (L > 0)$, we call corotating, and the circular orbits with $p^{(\varphi)} < 0,\ (L < 0)$ we call counterrotating, in agreement with the case of asymptotically flat Kerr spacetimes.

In the theory of accretion discs, the crucial property of circular orbits is their stability with respect to radial perturbations. Loci of stable circular orbits are given by the condition

$$\mathrm{d}^2R/\mathrm{d}r^2 \geq 0, \tag{1.24}$$

which has to be satisfied simultaneously with the conditions $R(r) = 0$ and $\mathrm{d}R/\mathrm{d}r = 0$ determining the circular orbits, and correspond to local minima of the effective potential $E_{(+)}$. (Local maxima of $E_{(+)}$ correspond to unstable circular orbits.) Stable (plus-family) circular orbits can exist only in the KdS spacetimes with the cosmological parameter

$$y \leq y_{\mathrm{c(ms+)}} = \frac{100}{(5+2\sqrt{10})^3} \doteq 0.069; \tag{1.25}$$

no stable circular orbits (of any family) exist for $y > y_{\mathrm{c(ms+)}}$. Critical value of the cosmological parameter for the existence of stable minus-family circular orbits corresponds to

$$y_{\mathrm{c(ms-)}} = \frac{12}{15^4} \doteq 0.00024 \tag{1.26}$$

and coincides with the limit on the existence of stable circular orbits in the SdS spacetimes [34]. Each family of orbits contains the innermost and the outermost stable circular orbit called the inner and the outer marginally stable orbit, $r_{\mathrm{ms(i)}}$ and $r_{\mathrm{ms(o)}}$, respectively, in between the stable circular orbits of a given family exist. Marginally stable orbits are determined by the equality in the relation (1.24).

Combined analysis of circular orbits with respect to the orientation and stability reveals that minus-family orbits (both stable and unstable) are always counterrotating from the point of view of LNRF. Plus-family orbits are usually corotating but counterrotating plus-family orbits also exist. In all (BH and NS) KdS backgrounds, the plus-family orbits become to be counterrotating in the vicinity of the upper limit for their existence (the static radius or the counterrotating photon circular orbit); these orbits are unstable. In naked-singularity backgrounds with the rotational parameter low enough (see Figure 1.2), the counterrotating plus-family circular orbits exist also in the vicinity of the ring singularity; these orbits are both unstable (located under the inner marginally stable orbit) and stable. For sufficiently high values of the cosmological parameter, $y \sim 0.06$, all stable plus-family orbits are counterrotating. Moreover, when the rotational parameter a is very close to the extreme-hole state, even counterrotating stable plus-family orbits with negative specific energy, $E_{+} < 0$, can exist (see Figure 1.2).

In the KdS spacetimes admitting stable circular orbits of a given family, the notion of the marginally bound orbits, i.e., unstable circular orbits where a small radial perturbation

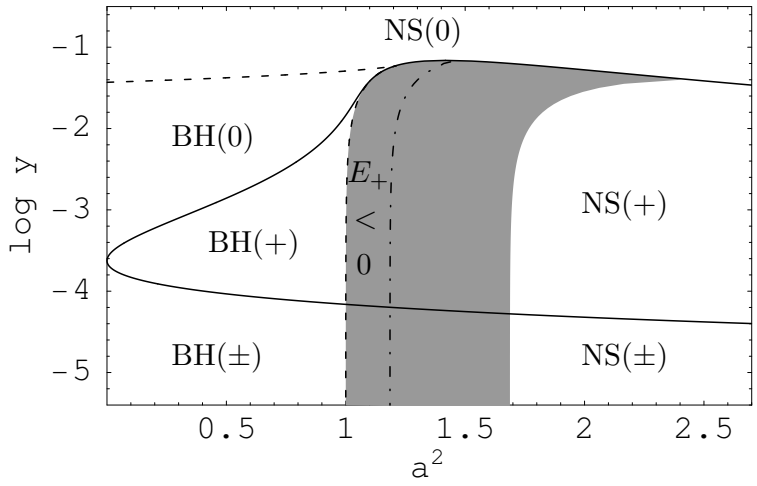

Figure 1.2: Separation of KdS spacetimes according to the existence of stable circular orbits of test particles in the equatorial plane. Dashed curve separates regions of black holes (BH) and naked singularities (NS), full curves separate spacetimes admitting either both families (±) of stable circular orbits, or the plus-family (+) only, or even no (0) stable circular orbits. For large values of a^2 both the full lines tend to the a^2-axis. Shaded region corresponds to the NS spacetimes admitting counterrotating stable plus-family orbits, dashed-dotted curve forms the boundary of subregion where these counterrotating stable plus-family orbits possess negative specific energy.

causes infall of a particle from the orbit to the center or its escape to the cosmological horizon, is introduced by the relation between the local maxima of the effective potential

$$E_{(+)}(r = r_{\mathrm{mb(i)}};\ X = X_{\mathrm{mb}},\ a,\ y) = E_{(+)}(r = r_{\mathrm{mb(o)}};\ X = X_{\mathrm{mb}},\ a,\ y), \tag{1.27}$$

determining the location of the inner and outer marginally bound orbit, $r_{\mathrm{mb(i)}}$ and $r_{\mathrm{mb(o)}}$; X_{mb} corresponds to special value of the axial parameter X resulting in the relation (1.27), see Figure 1.1.

Profile of the angular velocity $\Omega = \mathrm{d}\varphi/\mathrm{d}t$ of a thin, Keplerian accretion disc is given by

$$\Omega_{\mathrm{K}\pm} = \pm\frac{1}{r^{3/2}/(1 - yr^3)^{1/2} \pm a}. \tag{1.28}$$

Matter in the thin disc spirals from the outer edge located close to the outer marginally stable orbit, $r_{\mathrm{out}} \approx r_{\mathrm{ms(o)}}$, through the sequence of stable circular orbits down to the inner edge located on the inner marginally stable orbit, $r_{\mathrm{in}} \approx r_{\mathrm{ms(i)}}$, losing energy and angular momentum due to the viscosity. The necessary conditions for such a differential rotation,

$$\frac{\mathrm{d}\Omega_{\mathrm{K}+}}{\mathrm{d}r} < 0, \quad \frac{\mathrm{d}E_+}{\mathrm{d}r} \geq 0, \quad \frac{\mathrm{d}L_+}{\mathrm{d}r} \geq 0, \tag{1.29}$$

in the case of plus-family discs, or

$$\frac{\mathrm{d}\Omega_{\mathrm{K}-}}{\mathrm{d}r} > 0, \quad \frac{\mathrm{d}E_-}{\mathrm{d}r} \leq 0, \quad \frac{\mathrm{d}L_-}{\mathrm{d}r} \leq 0, \tag{1.30}$$

in the case of minus-family discs, are fulfilled by the relations (1.16)–(1.17) and (1.28). Maximum efficiency of accretion is thus given by the difference of specific energies of a particle on the outer and the inner marginally stable orbit,

$$\eta \equiv E_{\mathrm{ms(o)}} - E_{\mathrm{ms(i)}}. \tag{1.31}$$

For Keplerian discs corotating extreme KdS black holes, the accretion efficiency reaches maximum value of $\eta \sim 0.43$ for the pure Kerr case ($y = 0$) and tends to zero for $y \to y_{\mathrm{c(KdS)}} \doteq 0.059$, the maximum value of y admitting black holes. For plus-family discs orbiting the KdS naked singularity with the rotational parameter close to the extreme-hole state, $a \to a_{\mathrm{ex}}(y)$ for a given cosmological parameter $y < y_{\mathrm{c(KdS)}}$, the accretion efficiency usually exceeds the efficiency of annihilation processes, $\eta > 1$. Again, maximum value corresponds to the pure Kerr case ($y = 0$), $\eta \sim 1.57$ [32], and tends to zero for $y \to y_{\mathrm{c(KdS)}}$. Due to the strong discontinuity in properties of the plus-family orbits for extreme black holes and naked singularities with $a \to a_{\mathrm{ex}}(y)$, conversion of a naked singularity into an extreme black hole, induced by the accretion in plus-family discs, leads to an abrupt instability of the innermost parts of the discs that can have strong observational consequences.

1.2 Thick discs

Basic properties of thick discs are determined by the equilibrium toroidal configurations of perfect fluid orbiting in the background. Analytic theory of equilibrium configurations of rotating perfect fluid bodies was developed by Boyer [14] and than studied by many authors. The main result of the theory, known as "Boyer's condition", states that the boundary of any stationary, barotropic, perfect fluid body has to be an equipotential surface. Here we shall summarize its application to the relativistic test perfect fluid orbiting in a stationary and axisymmetric way in a stationary, axisymmetric background, as was introduced by Abramowicz and co-workers in the case of Schwarzschild and Kerr black holes [21, 4].

In the standard Boyer–Lindquist coordinates the spacetime is described by the line element

$$\mathrm{d}s^2 = g_{tt}\mathrm{d}t^2 + 2g_{t\varphi}\mathrm{d}t\mathrm{d}\varphi + g_{\varphi\varphi}\mathrm{d}\varphi^2 + g_{rr}\mathrm{d}r^2 + g_{\theta\theta}\mathrm{d}\theta^2 \tag{1.32}$$

satisfying the properties of stationarity and axial symmetry, i.e., $\partial_t g_{\mu\nu} = \partial_\varphi g_{\mu\nu} = 0$. The stress-energy tensor of perfect fluid is given by

$$T^{\mu}{}_{\nu} = (\epsilon + p)U^{\mu}U_{\nu} + p\,\delta^{\mu}_{\nu}, \tag{1.33}$$

where ϵ and p denote total energy density and pressure of the fluid. Further, we consider test perfect fluid moving in azimuthal direction only, i.e., its 4-velocity U^{μ} has two non-zero components,

$$U^{\mu} = (U^t,\ U^{\varphi},\ 0,\ 0), \tag{1.34}$$

which can be functions of the coordinates $r,\ \theta$ only. The rotating fluid can be characterized by the vector fields of the angular velocity $\Omega\ (r,\ \theta)$ and the specific angular momentum (angular momentum per unit *total* mass) $\ell\ (r,\ \theta)$, defined by

$$\Omega = \frac{U^{\varphi}}{U^t}, \qquad \ell = -\frac{U_{\varphi}}{U_t} \tag{1.35}$$

and related by the metric coefficients of the background

$$\Omega = -\frac{g_{t\varphi} + \ell g_{tt}}{g_{\varphi\varphi} + \ell g_{t\varphi}}. \tag{1.36}$$

Projecting the energy-momentum conservation law $\nabla_\nu T^{\mu\nu} = 0$ onto the hypersurface orthogonal to the 4-velocity U^μ by the projection tensor $h_{\mu\nu} = g_{\mu\nu} + U_\mu U_\nu$, we obtain the relativistic Euler equation in the axially symmetric form

$$\frac{\partial_i p}{\epsilon + p} = -\partial_i (\ln U_t) + \frac{\Omega\, \partial_i \ell}{1 - \Omega \ell}, \tag{1.37}$$

where $i = r,\ \theta$ and

$$(U_t)^2 = \frac{g_{t\varphi}^2 - g_{tt}\, g_{\varphi\varphi}}{g_{\varphi\varphi} + 2\ell g_{t\varphi} + \ell^2 g_{tt}}. \tag{1.38}$$

For a barotropic fluid, i.e., for a body with an equation of state $p = p(\epsilon)$, the surfaces of constant pressure are given, in accordance with Boyer's approach, by the equipotential surfaces of the potential $W(r,\ \theta)$ defined by the relations [4]

$$\int_0^p \frac{\mathrm{d}p}{\epsilon + p} = \ln(U_t)_{\rm in} - \ln(U_t) + \int_{\ell_{\rm in}}^{\ell} \frac{\Omega \mathrm{d}\ell}{1 - \Omega \ell} \equiv W_{\rm in} - W, \tag{1.39}$$

where the subscript "in" refers to the inner edge of the disc. The explicit form of the potential, $W = W(r,\ \theta)$, is given by the relations (1.38) and (1.39), if one specifies the metric tensor of the background and the "rotational law", i.e., the function $\Omega = \Omega(l)$. The simplest but also astrophysically very important is the case of uniform distribution of the specific angular momentum,

$$\ell(r,\ \theta) = \text{const}, \tag{1.40}$$

through the disc. It is well known that the tori with $\ell(r,\ \theta) = \text{const}$ are marginally stable [30] and capable to produce maximal luminosity at all [2]. Moreover, topological properties of the equipotential surfaces seem to be rather independent of the distribution of the specific angular momentum $\ell(r,\ \theta)$, see, e.g., [2, 19, 1]. In this special case the potential is given by very simple formula

$$W(r,\ \theta) = \ln U_t(r,\ \theta) \tag{1.41}$$

and is fully determined by the geometry of the background. Note that the points where $\partial_i W = 0$ correspond to free-particle (geodesic) motion due to the vanishing of the pressure-gradient forces there. Moreover, at the center of any perfect fluid torus the pressure attains the extreme value (maximum) and matter must follow a stable geodesic there. Thus, thick discs can exist only in the backgrounds allowing the motion along stable circular geodetical orbits.

Equipotential surfaces $\theta = \theta(r)$, determined by the condition $W(r,\ \theta) = \text{const}$, are given by the relation

$$\frac{\mathrm{d}\theta}{\mathrm{d}r} = -\frac{\partial p/\partial r}{\partial p/\partial \theta}, \tag{1.42}$$

which for the configurations with $\ell = \text{const}$ reduces to

$$\frac{\mathrm{d}\theta}{\mathrm{d}r} = -\frac{\partial U_t/\partial r}{\partial U_t/\partial \theta}. \tag{1.43}$$

The equipotential surfaces can be closed or open. Moreover, there is a special class of critical surfaces self-crossing in a cusp(s), which can be either marginally closed or open.

The closed—toroidal—equipotential surfaces determine stationary configurations (tori). The fluid can fill any toroidal equipotential surface; at the surface of the torus pressure vanishes, but its gradient is non-zero [21]. On the other hand, the open equipotential surfaces are important in dynamical situations, e.g., in modeling of jets [23, 12]. The critical—marginally closed—equipotential surfaces $W_{\rm crit}$ are important in the theory of thick accretion discs, because accretion onto the black hole through the cusp of the equipotential surface, located in the equatorial plane, is possible due to a little overcoming of the critical surface by the surface of the disc (Paczyński mechanism). Accretion is thus driven by a violation of the hydrostatic equilibrium, rather than by viscosity of the accreting matter [21].

In the KdS backgrounds, the potential (1.41) takes the form

$$W(r,\,\theta) = \ln\left\{\frac{\rho^2}{I^2}\frac{\Delta_r\Delta_\theta\sin^2\theta}{\Delta_\theta(r^2+a^2-a\ell)^2\sin^2\theta-\Delta_r(\ell-a\sin^2\theta)^2}\right\}^{1/2} \tag{1.44}$$

where

$$\rho^2 = r^2+a^2\cos^2\theta, \qquad \Delta_\theta = 1+ya^2\cos^2\theta. \tag{1.45}$$

Performing the limit $a\to 0$ we get the corresponding form of the potential (1.41) in the SdS backgrounds. All relevant properties of the equipotential surfaces are determined by behaviour of the potential in the equatorial plane ($\theta=\pi/2$). Inspecting the reality conditions of $W(r,\,\theta=\pi/2)$ in the stationary parts of the background ($\Delta_r\geq 0$; in the black-hole backgrounds, we again restrict our attention to the stationary region between the (outer) black-hole and cosmological horizon only), we arrive at the condition for the occurrence of matter with a given distribution of $\ell(r,\,\theta)$,

$$\ell_{\rm ph-} < \ell < \ell_{\rm ph+}, \tag{1.46}$$

where

$$\ell_{\rm ph\pm}(r;\,a,\,y) = a+\frac{r^2}{a\pm\sqrt{\Delta_r}} \tag{1.47}$$

corresponds to the effective potential of the photon geodesic motion; see [35] for an alternative definition. Local extrema of the function $W(r,\,\theta=\pi/2)$ lie at those radii where the specific angular momentum coincides with the specific angular momentum of test particles moving on the geodetical (Keplerian) circular orbits, i.e., where

$$\ell = \ell_{\rm K\pm}(r;\,a,\,y) \equiv \pm\frac{(r^2+a^2)(1-yr^3)^{1/2}\mp ar^{1/2}[2+r(r^2+a^2)y]}{r^{3/2}[1-(r^2+a^2)y]-2r^{1/2}\pm a(1-yr^3)^{1/2}}. \tag{1.48}$$

Those extrema are the only local extrema of the function $W(r,\,\theta)$.

Toroidal configurations arise for such a distribution of $\ell(r,\,\theta)$ in the disc which intersects the Keplerian distribution $\ell_{\rm K\pm}(r)$ in the part(s) corresponding to stable circular orbits. In black-hole backgrounds, stationary toroidal configurations exist for $\ell\in(\ell_{\rm ms(i)},\,\ell_{\rm ms(o)})$, where $\ell_{\rm ms(i)}$ ($\ell_{\rm ms(o)}$) corresponds to the Keplerian specific angular momentum on the inner (outer) marginally stable orbit. The same is true also in most of the naked-singularity backgrounds, however, exceptions exist concerning the plus-family discs in naked-singularity backgrounds with the rotational parameter low enough to admit counterrotating stable plus-family circular geodesics. In fact, there are naked-singularity backgrounds, in which the stationary tori exist for any uniform distribution of $\ell(r,\,\theta)$ in the disc.

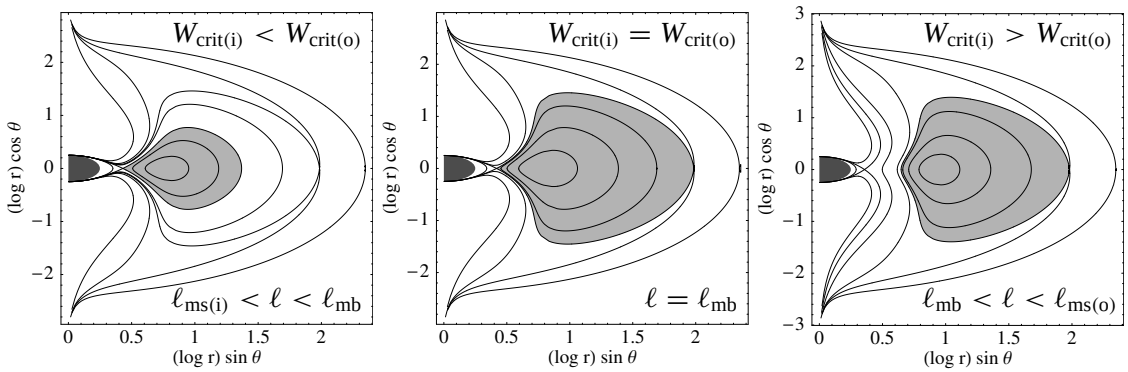

Figure 1.3: Typical behaviour of equipotential surfaces (meridional sections) in SdS and KdS black-hole spacetimes. Light gray region contains closed equipotential surfaces. The last closed surface is self-crossing in the cusp(s). Possible toroidal configurations correspond to: (a) accretion discs, (b) marginally bound accretion discs and (c) excretion discs.

In both black-hole and naked-singularity backgrounds we can distinguish three kinds of discs (Figure 1.3):

accretion discs: Toroidal equipotential surfaces are bounded by the marginally closed critical equipotential surface self-crossing in the inner cusp and enabling outflow of matter from the disc into the BH/NS. Another critical surface self-crossing in the outer cusp is open. Matter filling the region between the critical surfaces cannot remain in hydrostatic equilibrium and contributes to the accretion flow along the inner cusp and a throat formed by open surfaces. Moreover, if the potential levels corresponding to the critical surfaces are comparable, i.e., $W_{\mathrm{crit(i)}} \lesssim W_{\mathrm{crit(o)}}$, huge overfilling of the critical surface with the inner cusp causing the accretion could be combined with the so-called *excretion*, i.e., outflow through the outer cusp (after overfilling of the critical surface with the outer cusp), having a capability to regulate the accretion.

marginally bound accretion discs: Such configurations exist only for the uniform distribution of the specific angular momentum in the disc $\ell(r,\,\theta) = \ell_{\mathrm{mb}}$, where ℓ_{mb} corresponds to the Keplerian specific angular momentum on the marginally bound circular orbit. Toroidal equipotential surfaces are bounded by the marginally closed critical equipotential surface self-crossing in both the cusps. Any overfilling of the critical surface causes the accretion inflow through the inner cusp as well as the excretion outflow through the outer cusp.

excretion discs: Toroidal equipotential surfaces are bounded by the marginally closed critical equipotential surface self-crossing in the outer cusp and enabling outflow of matter from the disc into the outer space by a violation of hydrostatic equilibrium. The equipotential surface with the inner cusp, if such a surface exists, is open (cylindrical) and separated from the critical surface with the outer cusp by other cylindrical surfaces which, in fact, disable accretion into the black hole.

In KdS naked-singularity backgrounds allowing counterrotating stable plus-family circular orbits, some more exotic configurations exist:

a. counterrotating negative-energy discs

   Specific energy of the fluid elements in the center and the cusps (where the fluid follows the geodesic motion) is negative and we can expect that every fluid element in the disc has energy $E < 0$. Moreover, no open equipotential surfaces going out from the singularity are connected with such configurations. In the case of accretion discs, the equipotential surface with the outer cusp need not exist.

b. configurations with two isolated discs corresponding to the same value of ℓ

   The inner disc is always counterrotating accretion disc (with matter in the states with $E < 0$ or $E > 0$), the outer disc can be, in dependence on the value of ℓ, the corotating or counterrotating excretion disc, as well as the counterrotating accretion disc.

Due to the existence of non-zero pressure-gradients in the fluid, the inner edge of accretion discs (corresponding to the inner cusp of equipotential surfaces) is shifted under the inner marginally stable orbit up to the inner marginally bound orbit, $r_{\mathrm{mb(i)}} < r_{\mathrm{in}} < r_{\mathrm{ms(i)}}$. Similarly, the outer edge of excretion discs (corresponding to the outer cusp of equipotential surfaces) is located between the outer marginally stable and outer marginally bound orbit, $r_{\mathrm{ms(o)}} < r_{\mathrm{out}} < r_{\mathrm{mb(o)}}$. Marginally bound accretion discs have, thus, naturally determined both edges by the location of the cusps of the only critical surface, $r_{\mathrm{in}} \approx r_{\mathrm{mb(i)}}$, $r_{\mathrm{out}} \approx r_{\mathrm{mb(o)}}$, and correspond to maximally extended discs. Moreover, potential difference between the boundary (determined by the marginally closed critical surface) and the center of the torus, $\Delta W = W_{\mathrm{crit}} - W_{\mathrm{center}}$, takes the largest values for plus-family marginally bound accretion discs. In black-hole backgrounds, the maximal value corresponds to the disc corotating the extreme Kerr black hole ($y = 0$), $\Delta W \approx 0.549$ [4], and with the cosmological parameter y growing up to $y_{\mathrm{c(KdS)}} \doteq 0.059$ tends to zero. In naked-singularity backgrounds, the potential difference grows unlimitedly, $\Delta W \to \infty$, for the plus-family discs orbiting a naked singularity approaching the extreme-hole state, independently of the cosmological parameter $y < y_{\mathrm{c(KdS)}}$.

We conclude that in the structure and properties of equipotential surfaces, there are two qualitatively new features connected with a cosmic repulsion, which both take place nearby the static radius of a given spacetime. The first one is the outer cusp which enables the outflow of matter from the new type of stationary tori—the *excretion discs*. The outflow through the outer cusp is driven by the same mechanism as the outflow through the inner cusp in the case of accretion discs, i.e., by a violation of hydrostatic equilibrium. However, the outer cusp plays an important role also for the accretion discs, as puts an upper limit on their extension. Recall that no such an outer edge is naturally defined in the case of accretion discs orbiting a single black hole (naked singularity) in asymptotically flat Schwarzschild or Kerr backgrounds. Moreover, as shown by Rezzolla *et al* [29] in the case of perfect fluid tori orbiting SdS black holes, excretion outflow through the outer cusp could stabilize the accretion discs against the so-called *runaway instability* [3].

The second feature connected with the cosmic repulsion consists in strong collimation of open equipotential surfaces near the axis of rotation, being evident nearby and behind the static radius, when compared with the Kerr case, suggesting a certain role of $\Lambda > 0$ in the collimation of jets far away from the maternal accretion or excretion disc. See Figure 1.4 (left) comparing the cases with or without the cosmic repulsion.

Rotation of the background influences the shape of tori: the corotating discs are thicker and more extended than the counterrotating ones, generating narrower funnel

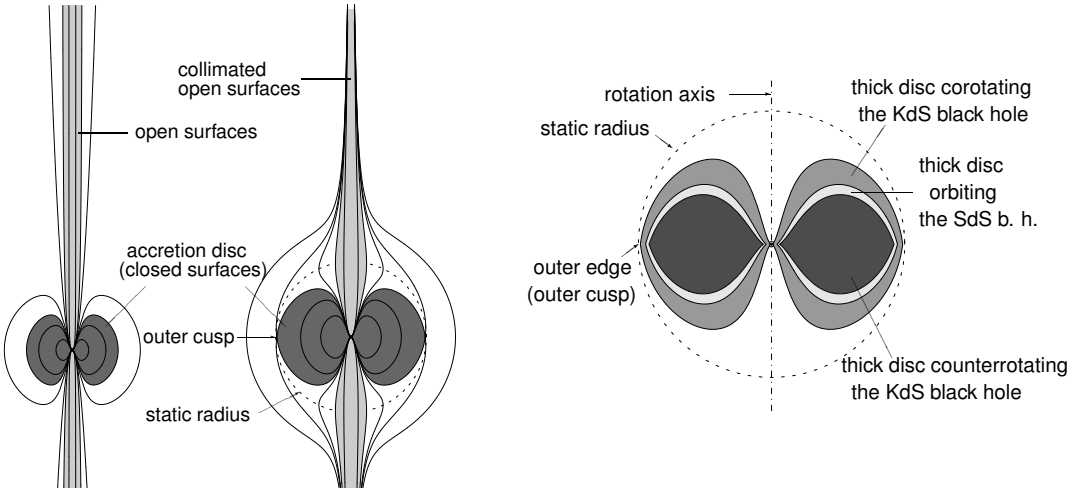

Figure 1.4: (left) Influence of a repulsive cosmological constant on the structure of equipotential surfaces. Configurations corresponding to accretion discs corotating the Kerr ($y = 0,\ a^2 = 0.99$) and the KdS ($y = 10^{-6},\ a^2 = 0.99$) black hole are compared. (right) Influence of spacetime's rotation on the shape of marginally bound accretion discs ($\ell = \ell_{\rm mb}$) orbiting the KdS black hole ($y = 10^{-6},\ a^2 = 0.99$). For comparison, thick marginally bound accretion disc orbiting the SdS black hole ($y = 10^{-6},\ a = 0$) is presented.

Table 1.1: Mass parameter, the static radius and radius of the outer marginally stable orbit in extreme KdS black-hole spacetimes are given for the current value of the cosmological constant, $\Lambda_0 \approx 1.3 \times 10^{-56}\ \mathrm{cm}^{-2}$.

y	10^{-44}	10^{-42}	10^{-34}	10^{-30}	10^{-28}	10^{-26}	10^{-22}
$M/M_\odot$	10	100	10^6	10^8	10^9	10^{10}	10^{12}
$r_{\rm s}$/[kpc]	0.2	0.5	11	50	110	230	1100
$r_{\rm ms}$/[kpc]	0.15	0.3	6.7	31	67	150	670

where highly collimated relativistic streams of particles—jets are most probably created [17]. In Figure 1.4 (right) the shapes of marginally bound accretion discs corotating/counterrotating the KdS black hole are compared with the marginally bound accretion disc orbiting the SdS black hole (corresponding to the same value of the cosmological parameter y).

Finally, we shall give an idea on scales, at which the discussed effects take place, by expressing basic characteristics of the tori in astrophysical units for the current value of the cosmological constant, $\Lambda = \Lambda_0$. The results are presented in Table 1.1. As the outer edge of tori is located between the outer marginally stable orbit and the static radius, $r_{\rm ms(o)} < r_{\rm out} < r_{\rm s}$, the repulsive cosmological constant puts a limit on maximal extension of disc-like structures in a given background. Remarkably but rather by coincidence, for supermassive black holes ($10^6 M_\odot$–$10^{10} M_\odot$), the dimensions of *test* tori are roughly comparable with the dimensions of galaxies [15]. Of course, to get a more realistic picture, influence of the cosmic repulsion on self-gravitating tori has to be studied. On the other hand, since the jets escaping from AGN can many times exceed the dimension of the galaxy, repulsive cosmological constant could play an important role in the collimation of jets far away from the "seed" galaxy.

2

Aschenbach effect

Aschenbach [7] found a very interesting and rather surprising fact about the circular orbits of free particles around the Kerr black holes with high spin: contrary to what is true for Kerr black holes with a small spin, for orbits around the Kerr black holes with $a > 0.9953$ the Keplerian orbital velocity $\mathcal{V}_{\mathrm{K}}^{(\varphi)}$ measured in locally non-rotating frames (LNRF) is a non-monotonic function of radius. Moreover, Aschenbach proposed that excitation of oscillations in Keplerian thin discs can be related to this fact.[1]

The locally non-rotating frames are given by the tetrad of 1-forms [11]

$$\omega^{(t)} \equiv \left(\frac{\Sigma\Delta}{A}\right)^{1/2} \mathrm{d}t, \quad \omega^{(\varphi)} \equiv \left(\frac{A}{\Sigma}\right)^{1/2} \sin\theta(\mathrm{d}\varphi - \Omega_{\mathrm{LNRF}}\,\mathrm{d}t), \tag{2.1}$$

$$\omega^{(r)} \equiv \left(\frac{\Sigma}{\Delta}\right)^{1/2} \mathrm{d}r, \qquad \omega^{(\theta)} \equiv \Sigma^{1/2}\mathrm{d}\theta \tag{2.2}$$

where

$$\Delta = r^2 - 2r + a^2, \quad \Sigma = r^2 + a^2\cos^2\theta, \quad A = (r^2+a^2)^2 - \Delta\, a^2 \sin^2\theta \tag{2.3}$$

and the angular velocity of LNRF, $\Omega_{\mathrm{LNRF}} \equiv -g_{t\varphi}/g_{\varphi\varphi}$, is given by the relation

$$\Omega_{\mathrm{LNRF}} = \frac{2ar}{A}. \tag{2.4}$$

The orbital velocity of matter in the disc moving with the 4-velocity U^μ corresponds to the azimuthal component of its 3-velocity in LNRF given by

$$\mathcal{V}^{(\varphi)} = \frac{U^\mu \omega_\mu^{(\varphi)}}{U^\nu \omega_\nu^{(t)}} = \frac{A\sin\theta}{\Sigma\sqrt{\Delta}}(\Omega - \Omega_{\mathrm{LNRF}}). \tag{2.5}$$

where $\Omega = \mathrm{d}\varphi/\mathrm{d}t$ is the angular velocity of the disc. Substituting for Ω the angular velocity of Keplerian motion in corotating thin discs,

$$\Omega_{\mathrm{K}}(r) = \frac{1}{(r^{3/2}+a)}, \tag{2.6}$$

[1] Units $c = G = M = 1$ and Boyer–Lindquist coordinates $(t,\ r,\ \theta,\ \varphi)$ are used hereafter.

we arrive at the formula for Keplerian orbital velocity analyzed by Aschenbach

$$\mathcal{V}_{\rm K}^{(\varphi)}(r) = \frac{(r^2+a^2)^2 - a^2\Delta - 2ar(r^{3/2}+a)}{r^2(r^{3/2}+a)\sqrt{\Delta}}. \tag{2.7}$$

In paper [**IV**] we analyzed the orbital velocity of perfect fluid tori with uniform distribution of the specific angular momentum, $\ell(r,\,\theta) = \text{const}$, corotating a Kerr black hole, and found that there is a corresponding change of behaviour of the orbital velocity also for non-Keplerian motion in thick discs.

The angular velocity of thick discs is given by the relation (1.36) which in Kerr backgrounds takes the form

$$\Omega = \Omega(r,\,\theta) = \frac{(\Delta - a^2\sin^2\theta)\ell + 2ar\sin^2\theta}{(A - 2\ell ar)\sin^2\theta}. \tag{2.8}$$

Successively, we arrive at the formula for orbital velocity of marginally stable ($\ell = \text{const}$) perfect-fluid tori

$$\mathcal{V}^{(\varphi)}(r,\,\theta) = \frac{A(\Delta - a^2\sin^2\theta) + 4a^2r^2\sin^2\theta}{\Sigma\sqrt{\Delta}(A - 2a\ell r)\sin\theta}\ell, \tag{2.9}$$

which in the equatorial plane, $\theta = \pi/2$, reduces to

$$\mathcal{V}^{(\varphi)}(r,\,\theta=\pi/2) = \frac{r\sqrt{\Delta}}{r(r^2+a^2) - 2a(\ell - a)}\ell. \tag{2.10}$$

Analyzing the function (2.10) in terms of the existence of local extrema we found that one local extreme (maximum) exists for *any* pair of $(a,\,\ell)$. Moreover, if the spin of a Kerr black hole is sufficiently large,

$$a > a_{\rm c(bh)} \doteq 0.99964, \tag{2.11}$$

other two local extrema (maximum and minimum) arise for appropriately chosen specific angular momentum ℓ of the disc, and the radial gradient, $\partial\mathcal{V}^{(\varphi)}/\partial r$, changes its sign three times. Note that the same effect exists also in Kerr naked-singularity spacetimes with the rotational parameter

$$1 < a < a_{\rm c(ns)} \doteq 1.50429. \tag{2.12}$$

Next we shall consider marginally stable thick discs orbiting the Kerr black holes only.

It was shown by Abramowicz *et al* [4] that the barotropic perfect-fluid tori with uniform distribution of the specific angular momentum, $\ell(r,\,\theta) = \text{const}$, corresponding to thick accretion discs, exist if $\ell_{\rm ms} < \ell < \ell_{\rm mb}$, where $\ell_{\rm ms}$ and $\ell_{\rm mb}$ denotes the specific angular momentum of test particles on marginally stable and marginally bound orbit, respectively. Moreover, the inner edge of the disc, determined by the cusp of equipotential surfaces in the fluid, is located between the marginally bound and marginally stable orbit, $r_{\rm mb} < r_{\rm in} < r_{\rm ms}$. Taking these results into account we conclude that the *Aschenbach effect*, connected with a non-monotonic behaviour of the orbital velocity $\mathcal{V}^{(\varphi)}$ of the disc related to the LNRF, can exist in marginally stable perfect-fluid tori orbiting the Kerr black holes with spin

$$a > a_{\rm c(tori)} \doteq 0.99979, \tag{2.13}$$

which is much closer to the extreme-hole state than the critical value $a_{\mathrm{c(K)}} \doteq 0.9953$ determined by Aschenbach for Keplerian discs [7]. Positive radial gradient of the orbital velocity occurs just above the center of the tori, in the region where stable equatorial circular geodesics of given Kerr spacetime are allowed. Note that the first, always existing local maximum of $\mathcal{V}^{(\varphi)}$ is always located outside the disc, under its inner edge. The difference of locally measured orbital velocities at local maximum and local minimum of $\mathcal{V}^{(\varphi)}$, $\Delta\mathcal{V}^{(\varphi)} \equiv \mathcal{V}^{(\varphi)}_{\mathrm{max}} - \mathcal{V}^{(\varphi)}_{\mathrm{min}}$, grows with spin of the black hole, reaching maximal value for the extreme Kerr black hole ($a = 1,\ \ell = 2$), $\Delta\mathcal{V}^{(\varphi)}_{\mathrm{tori}} \approx 0.02$, which is smaller but comparable with maximal value for Keplerian discs, $\Delta\mathcal{V}^{(\varphi)}_{\mathrm{K}} \approx 0.07$. These are really huge velocity differences, being expressed in units of c.

Global character of the phenomenon outside the equatorial plane is manifested by behaviour of von Zeipel surfaces. Rotational properties of barotropic perfect-fluid bodies in strong gravity are well represented by the radius of gyration $\widehat{\mathcal{R}}$, introduced in the case of spherically symmetric Schwarzschild spacetimes in [5], as the direction of increase of $\widehat{\mathcal{R}}$ defines a local outward direction of the dynamical effects of rotation of the fluid. In the stationary and axisymmetric spacetimes, the definition of the radius of gyration was generalized [6] so that $\mathcal{V}^{(\varphi)} = \widehat{\Omega}\widehat{\mathcal{R}}$, where $\widehat{\Omega} = \Omega - \Omega_{\mathrm{LNRF}}$. Here we shall use another physically reasonable way of how to define a global quantity characterizing rotating fluid configurations. We define so-called von Zeipel radius by the relation

$$\mathcal{R}(r,\ \theta) \equiv \frac{\ell(r,\ \theta)}{\mathcal{V}^{(\varphi)}(r,\ \theta)} \tag{2.14}$$

which generalizes the Schwarzschildian definition of gyration radius. In static spacetimes, the von Zeipel radius (2.14) coincides with the radius of gyration, however, in stationary, axisymmetric spacetimes, relation between the both radii has the form

$$\mathcal{R} = (1 - \Omega_{\mathrm{LNRF}}\,\ell)\widehat{\mathcal{R}}. \tag{2.15}$$

In the case of tori with $\ell(r,\ \theta) = \mathrm{const}$, the von Zeipel surfaces, i.e., the surfaces of $\mathcal{R}(r,\ \theta) = \mathrm{const}$, coincide with the equivelocity surfaces $\mathcal{V}^{(\varphi)}(r,\ \theta) = \mathrm{const}$. It is shown that the *Aschenbach effect* is connected with topology changes of the von Zeipel surfaces. In addition to the open surface crossing itself under the inner edge of the torus and existing for all values of the rotational parameter a, for $a > a_{\mathrm{c(tori)}}$ the second self-crossing (marginally closed) surface together with toroidal surfaces occur. Toroidal von Zeipel surfaces exist under the newly developing cusp, being centered around the circle corresponding to the minimum of the equatorial LNRF velocity profile, see Figure 2.1. The whole effect, elucidated by toroidal von Zeipel surfaces, is located inside the ergosphere of a given Kerr spacetime.

Toroidal equivelocity surfaces bounded by the marginally closed surface with a cusp could induce some vertical and/or vortical instabilities causing, eventually, local oscillations of the disc. In accordance with Aschenbach [7], we can define the typical frequency of the mechanism for excitation of oscillations by the maximum slope of the positive gradient of $\partial\mathcal{V}^{(\varphi)}/\partial r$ in between the changes of its sign in the equatorial plane,

$$\Omega_{\mathrm{osc}} = 2\pi\frac{\partial\mathcal{V}^{(\varphi)}}{\partial r}|_{\mathrm{max}}. \tag{2.16}$$

However, for estimation of physically realistic characteristic frequencies related to local physics in the disc, the radial gradient related to *proper* (coordinate-independent) radial

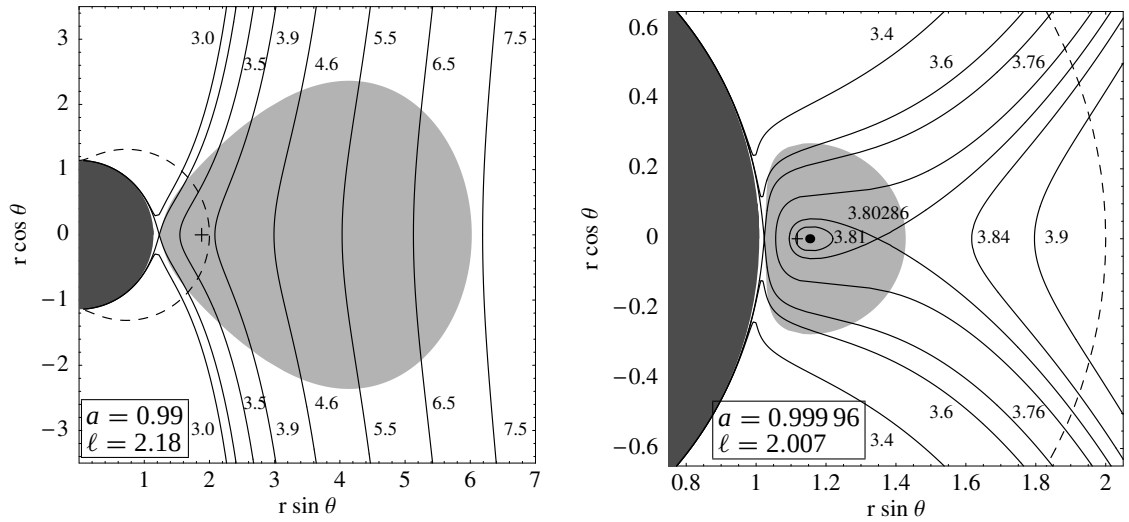

(a) (b)

Figure 2.1: Von Zeipel (equivelocity) surfaces in thick accretion discs (shaded region) with uniform distribution of the specific angular momentum close to the one at the marginally stable circular geodesic. Dashed curve corresponds to the ergosphere, cross denotes the center of the disc. (a) just open (cylindrical) surfaces exist in the disc. (b) toroidal surfaces exist in the region near the center of the disc; $\mathcal{R}_{\rm ring} \doteq 3.814$

distance,

$$\mathrm{d}\tilde{r} = \sqrt{g_{rr}}\mathrm{d}r = \sqrt{\frac{\Sigma}{\Delta}}\mathrm{d}r, \tag{2.17}$$

seems to be more appropriate. In terms of the proper radial distance, the critical frequency for possible excitation of oscillations is given by the relation

$$\tilde{\Omega}_{\rm osc} = 2\pi \frac{\partial \mathcal{V}^{(\varphi)}}{\partial \tilde{r}}|_{\rm max}. \tag{2.18}$$

As the frequencies (2.16) and (2.18) are related to the LNRF, it is useful to relate the frequencies also to the static observer at radial infinity. Corresponding formulae are given by the relations

$$\Omega_\infty = \sqrt{-(g_{tt} + 2\Omega_{\rm LNRF}\, g_{t\varphi} + \Omega^2_{\rm LNRF}\, g_{\varphi\varphi})}\, \Omega_{\rm osc}, \tag{2.19}$$

$$\tilde{\Omega}_\infty = \sqrt{-(g_{tt} + 2\Omega_{\rm LNRF}\, g_{t\varphi} + \Omega^2_{\rm LNRF}\, g_{\varphi\varphi})}\, \tilde{\Omega}_{\rm osc}, \tag{2.20}$$

where g_{tt}, $g_{t\varphi}$ and $g_{\varphi\varphi}$ are particular metric coefficients of the Kerr geometry. While the frequencies (2.16) and (2.18) monotonically grow with the spin of a black hole for both Keplerian discs and marginally stable fluid tori, frequencies (2.19) and (2.20) reach the maximum for a certain spin $a < 1$; for Keplerian thin discs, the maximum frequency related to the static observer at infinity is approximately $97\,(M/M_\odot)^{-1}$ Hz, whereas for marginally stable tori, this is approximately $24\,(M/M_\odot)^{-1}$ Hz; $(M/M_\odot)$ is the mass of the Kerr BH in units of mass of the Sun.

Note, however, that a physical mechanism generating eventual oscillations and/or instabilities in the discs, connected with the *Aschenbach effect*, is unknown and the issue needs further investigation.

References

[1] M. A. Abramowicz. Physics of black hole accretion. In M. A. Abramowicz, G. Björnsson, and J. E. Pringle, editors, *Theory of Black Hole Accretion Disks*, page 50, Cambridge, 1998. Cambridge University Press.

[2] M. A. Abramowicz, M. Calvani, and L. Nobili. Thick accretion disks with super-Eddington luminosities. *Astrophys. J.*, 242:772, 1980.

[3] M. A. Abramowicz, M. Calvani, and L. Nobili. Runaway instability in accretion disks orbiting black holes. *Nature*, 302:597, 1983.

[4] M. A. Abramowicz, M. Jaroszyński, and M. Sikora. Relativistic, accreting disks. *Astronomy and Astrophysics*, 63:221, 1978.

[5] M. A. Abramowicz, J. Miller, and Z. Stuchlík. Concept of radius of gyration in general relativity. *Phys. Rev. D*, 47(4):1440, 1993.

[6] M. A. Abramowicz, P. Nurowski, and N. Wex. Optical reference geometry for stationary and axially symmetric spacetimes. *Classical Quantum Gravity*, 12(6):1467, 1995.

[7] B. Aschenbach. Measuring mass and angular momentum of black holes with high-frequency quasi-periodic oscillations. *Astronomy and Astrophysics*, 425:1075, 2004.

[8] N. Bahcall, J. P. Ostriker, S. Perlmutter, and P. J. Steinhardt. The cosmic triangle: Revealing the state of the universe. *Science*, 284:1481, 1999.

[9] J. M. Bardeen. Timelike and null geodesics in the Kerr metric. In C. De Witt and B. S. De Witt, editors, *Black Holes*, page 215, New York–London–Paris, 1973. Gordon and Breach.

[10] J. M. Bardeen and J. A. Petterson. The Lense–Thirring effect and accretion disks around Kerr black holes. *Astrophys. J. Lett.*, 195:L65, 1975.

[11] J. M. Bardeen, W. H. Press, and S. A. Teukolsky. Rotating black holes: locally nonrotating frames, energy extraction, and scalar synchrotron radiation. *Astrophys. J.*, 178:347, 1972.

[12] R. D. Blandford. Astrophysical black holes. In S. W. Hawking and W. Israel, editors, *Three hundred years of gravitation*, page 277, Cambridge, 1987. Cambridge University Press.

[13] R. D. Blandford. Physical processes in active galactic nuclei. In T. J.-L. Courvoisier and M. Mayor, editors, *Active Galactic Nuclei. Saas-Fee Advanced Course 20, Lectures Notes 1990*, page 161, Berlin, 1990. Swiss Society for Astrophysics and Astronomy, Springer-Verlag.

[14] R. H. Boyer. *Proc. Cambridge Phil. Soc.*, 61:527, 1965.

[15] B. W. Carroll and D. A. Ostlie. *An Introduction to Modern Astrophysics*. Addison-Wesley, Reading, Massachusetts, 1996.

[16] B. Carter. Black hole equilibrium states. In C. De Witt and B. S. De Witt, editors, *Black Holes*, page 57, New York–London–Paris, 1973. Gordon and Breach.

[17] J. Frank, A. King, and D. Raine. *Accretion Power in Astrophysics*. Cambridge University Press, 2002. 3rd edition.

[18] V. P. Frolov and I. D. Novikov. *Black Hole Physics*. Kluwer Academic Publishers, P.O. Box 17, 3300 AA Dordrecht, The Netherlands, 1998.

[19] M. Jaroszyński, M. A. Abramowicz, and B. Paczyński. Supercritical accretion disks around black holes. *Acta Astronom.*, 30:1, 1980.

[20] E. W. Kolb and M. S. Turner. *The Early Universe*. Addison-Wesley, Redwood City, California, 1990. The Advanced Book Program.

[21] M. Koz lowski, M. Jaroszyński, and M. A. Abramowicz. The analytic theory of fluid disks orbiting the Kerr black hole. *Astronomy and Astrophysics*, 63:209, 1978.

[22] K. Lake and T. Zannias. Naked singularities in self-similar gravitational collapse. *Phys. Rev. D*, 41(12):3866, 1990.

[23] D. Lynden-Bell. Galactic nuclei as collapsed old quasars. *Nature*, 223:690, 1969.

[24] J. C. Miller and F. de Felice. Gravitational collapse and rotation. I - Mass shedding and reduction of the a/m ratio. *Astrophys. J.*, 298:474, 1985.

[25] J. C. Miller and F. de Felice. Gravitational collapse and rotation. II - Gravitational radiation and reduction of the a/m ratio. *Astrophys. J.*, 298:480, 1985.

[26] I. F. Mirabel and L. F. Rodríguez. Microquasars in our Galaxy. *Nature*, 392:673, 1998.

[27] I. D. Novikov and K. S. Thorne. Black hole astrophysics. In C. De Witt and B. S. De Witt, editors, *Black Holes*, page 343, New York–London–Paris, 1973. Gordon and Breach.

[28] R. Penrose. Gravitational collapse: The role of general relativity. *Nuovo Cimento B*, 1(special number):252, 1969.

[29] L. Rezzolla, O. Zanotti, and J. A. Font. Dynamics of thick discs around Schwarzschild-de Sitter black holes. *Astronomy and Astrophysics*, 412:603, 2003.

[30] F. H. Seguin. The stability of nonuniform rotation in relativistic stars. *Astrophys. J.*, 197:745, 1975.

[31] D. N. Spergel et al. First Year Wilkinson Microwave Anisotropy Probe (WMAP) Observations: Determination of Cosmological Parameters. *Astrophys. J. Suppl.*, 148:175, 2003.

[32] Z. Stuchlík. Equatorial circular orbits and the motion of the shell of dust in the field of a rotating naked singularity. *Bull. Astronom. Inst. Czechoslovakia*, 31(3):129, 1980.

[33] Z. Stuchlík. The motion of test particles in black-hole backgrounds with non-zero cosmological constant. *Bull. Astronom. Inst. Czechoslovakia*, 34(3):129, 1983.

[34] Z. Stuchlík and S. Hledík. Some properties of the Schwarzschild–de Sitter and Schwarzschild–anti-de Sitter spacetimes. *Phys. Rev. D*, 60(4):044006, 1999.

[35] Z. Stuchlík and S. Hledík. Equatorial photon motion in the Kerr–Newman spacetimes with a non-zero cosmological constant. *Classical Quantum Gravity*, 17(21):4541, November 2000.

Appendix A

List of publications and conference contributions

Papers

[1] Z. Stuchlík, **P. Slaný** and S. Hledík: *Equilibrium configurations of perfect fluid orbiting Schwarzschild–de Sitter black holes*, Astronomy and Astrophysics **363**, 425 (2000).

cited in: L. Rezzolla, O. Zanotti and J. A. Font: *Dynamics of thick discs around Schwarzschild–de Sitter black holes*, Astronomy and Astrophysics **412**, 603 (2003).

[2] Z. Stuchlík and **P. Slaný**: *Equatorial circular orbits in the Kerr–de Sitter spacetimes*, Physical Review D **69**, 064001 (2004).

cited in: N. Cruz, M. Olivares and J. R. Villanueva: *The geodesic structure of the Schwarzschild–anti de Sitter black hole*, Classical and Quantum Gravity **22(6)**, 1167 (2005).

Z. Gu and H. Cheng: *The evolution of cosmic string loops in Kerr–de Sitter spacetimes*, arXiv: `hep-th/0412297` (2004).

S. Setiawan: *A short note on climbing gravity improbable: Superradiant ring fellowship of launching the high Lorentz-factor outflows/jets*, arXiv: `astro-ph/0506557` (2005).

[3] Z. Stuchlík, **P. Slaný**, G. Török and M. A. Abramowicz: *Aschenbach effect: Unexpected topology changes in the motion of particles and fluids orbiting rapidly rotating Kerr black holes*, Physical Review D **71**, 024037 (2005).

[4] **P. Slaný** and Z. Stuchlík: *Relativistic thick discs in the Kerr–de Sitter backgrounds*, Classical and Quantum Gravity **22**, 3623 (2005), *in press*.

Proceedings

[5] **P. Slaný**: *Some aspects of Kerr–de Sitter spacetimes relevant for accretion processes*, in Proceedings of *RAGtime 2/3: Workshops on black holes and neutron stars*,

Opava, 11–13/8–10 October 2000/01, S. Hledík and Z. Stuchlík, editors, Silesian University in Opava, Czech Republic, 2001, pp. 119–127.

[6] Z. Stuchlík and **P. Slaný**: *Accretion disks in the Kerr–de Sitter spacetimes*, in Proceedings of *RAGtime 4/5: Workshops on black holes and neutron stars, Opava, 14–16/13–15 October 2002/03*, S. Hledík and Z. Stuchlík, editors, Silesian University in Opava, Czech Republic, 2004, pp. 205–237.

[7] Z. Stuchlík, **P. Slaný** and G. Török: *Marginally stable thick discs with gradient inversion of orbital velocity measured in locally non-rotating frames (A mechanism for excitation of oscillations in accretion discs?)*, in Proceedings of *RAGtime 4/5: Workshops on black holes and neutron stars, Opava, 14–16/13–15 October 2002/03*, S. Hledík and Z. Stuchlík, editors, Silesian University in Opava, Czech Republic, 2004, pp. 239–256.

Workshops and conferences

RAGtime (annual workshops) Silesian University in Opava, Czech Republic: from 2000—regular participant, from 2001—regular talk on current research activities concerning the influence of a repulsive cosmological constant on accretion discs.

Compact Relativity meeting (workshop) 11/2003, Charles University in Prague, Czech Republic: *Some remarks on accretion disks*, talk.

Relativity miniworkshop 11/2004, Charles University in Prague, Czech Republic: *Orbital velocity in locally non-rotating frames*, talk.

VI. SIGRAV Graduate School (school+workshop) 17.–21. 5. 2005, Como, Italy: *Aschenbach effect*, talk.

GR17 (International conference on general relativity and gravitation) 18. –24. 7. 2004, Dublin, Ireland:
Z. Stuchlík and **P. Slaný**, *Relativistic discs orbiting the Kerr–de Sitter black holes*, poster.

Albert Einstein Century (conference) 18. –22. 7. 2005, Paris, France:

i. Z. Stuchlík, **P. Slaný** and G. Török, *Toroidal LNRF-velocity profiles in thick accretion discs orbiting rapidly rotating Kerr black holes*, oral presentation,

ii. Z. Stuchlík and **P. Slaný**, *Basic properties of toroidal structures in Kerr–de Sitter backgrounds*, oral presentation (Z.S.).